Geology

Crust and upper mantle electrical conductivity beneath the Yellowstone Hotspot Track

A. Kelbert, G. D. Egbert and C. deGroot-Hedlin

Email alerting services	click www.gsapubs.org/cgi/alerts to receive free e-mail alerts when new articles cite this article
Subscribe	click www.gsapubs.org/subscriptions/ to subscribe to Geology
Permission request	click http://www.geosociety.org/pubs/copyrt.htm#gsa to contact GSA

Notes

THE
GEOLOGICAL
SOCIETY
OF AMERICA

Crust and upper mantle electrical conductivity beneath the Yellowstone Hotspot Track

A. Kelbert[1], G. D. Egbert[1], and C. deGroot-Hedlin[2]
[1]College of Earth, Ocean and Atmospheric Sciences, Oregon State University, 104 CEOAS Admin Building, Corvallis, Oregon 97331, USA
[2]Scripps Institution of Oceanography, University of California–San Diego, La Jolla, California 92037, USA

ABSTRACT

Combining long-period magnetotelluric data from the spatially uniform EarthScope USArray and higher-resolution profiles, we obtain a regional three-dimensional electrical resistivity model in the Snake River Plain and Yellowstone areas (Idaho and Wyoming, United States), and provide new constraints on the large-scale distribution of melt and fluids beneath the Yellowstone hotspot track. Contrary to what would be expected from standard mantle plume models, the electromagnetic data suggest that there is little or no melt in the lower crust and upper mantle directly beneath Yellowstone caldera. Instead, low mantle resistivities (10 Ωm and below), which we infer to result from 1%–3% partial melt, are found 40–80 km beneath the eastern Snake River Plain, extending at least 200 km southwest of the caldera, beneath the area of modern basaltic magmatism. The reduced resistivities extend upward into the mid-crust primarily around the edges of the Snake River Plain, suggesting upward migration of melt and/or fluid is concentrated in these areas. The anomaly also shallows toward Yellowstone, where higher temperatures enhance permeability and allow melts to ascend into the crust. The top of the conductive layer is at its shallowest, in the upper crust, directly beneath the modern Yellowstone supervolcano.

INTRODUCTION

The Snake River Plain–Yellowstone (Idaho and Wyoming, United States) volcanic province has long been associated with a stationary deep mantle plume source (e.g., Hadley et al., 1976; Geist and Richards, 1993). However, this simple model is difficult to reconcile with at least some important observations of the system, including the temporal persistence of basaltic volcanism and geochemistry of erupted magmas, and the spatial and temporal relationship of magmatism in the Snake River Plain (SRP), Yellowstone, and High Lava Plains, leading some to emphasize the role of shallower lithospheric convection (e.g., Humphreys et al., 2000; Christiansen et al., 2002; Leeman et al., 2009).

While body-wave tomography images for this area are in broad agreement, they have been interpreted to support both plume and "no plume" hypotheses. Early studies based on local arrays suggested a continuous low-velocity plume beneath Yellowstone, dipping to the northwest and extending to at least the transition zone (e.g., Yuan and Dueker, 2005). Resolution has been greatly improved with the deployment of the USArray (a component of the EarthScope project), revealing that this low-velocity feature extends into the lower mantle, but is discontinuous (e.g., Tian et al., 2011; James et al., 2011).

USArray seismic data also provide a regional context for the Yellowstone low-velocity anomaly. Several studies have identified a broad volume devoid of fast anomalies extending through the transition zone into the uppermost lower mantle: a "slab gap" between segments of the subducting Juan de Fuca plate (Tian et al., 2011). Relatively low velocities within the gap have been interpreted as evidence for interaction with a deeper plume source (e.g., Obrebski et al., 2010; Tian et al., 2011), or mantle upwelling through the gap in response to a sinking slab segment (James et al., 2011).

Surface wave inversions of USArray data show fast anomalies beneath the eastern SRP and Yellowstone at mid- to lower crustal depths (except directly beneath and near the Yellowstone caldera), but a very pronounced low-velocity anomaly in the mantle between the Moho and 200 km depth, extending southwest from Yellowstone caldera in the direction of North American plate motion (Obrebski et al., 2010; Wagner et al., 2010; Gao et al., 2011; Yang et al., 2011).

MAGNETOTELLURIC DATA

Long-period magnetotelluric (MT) data have also been collected as part of USArray project, using the same 70 km site spacing as the seismic component. These data are highly sensitive to the presence of volatiles and partial melt, and thus offer potentially valuable additional constraints on the physical state of the crust and mantle in this tectonically and magmatically active area. Here we use recently developed three-dimensional (3-D) inversion methods to interpret long-period MT data from 91 USArray MT sites, covering much of Idaho and Wyoming, southern Montana, eastern Oregon, and northern Nevada, together with 32 sites from an earlier MT survey, collected in two denser profiles along (~40 km site spacing) and across (~10 km site spacing) the eastern SRP (see Fig. 1).

For 3-D inversion, we employed the Modular system for Electromagnetic Inversion (ModEM; Egbert and Kelbert, 2012), a flexible system for regularized inversion of electromagnetic data. In our application to the MT data, we regularized with a model covariance that penalizes deviations from a prior model, fitting all six MT data components from 123 sites, at 14 periods from 7.3 s to 5.2 h. Poor-quality data (~1%) were removed from the data set, and an error floor
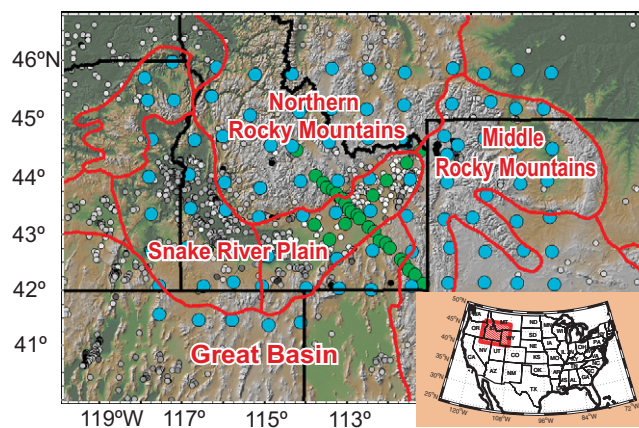
Figure 1. Topography of study area (see inset map for location within the United States), with physiographic provinces outlined in red. USArray magnetotelluric (MT) site locations used for this study are marked with blue dots; 32 sites from the earlier Snake River Plain profiles are denoted by green dots. Smaller gray dots indicate heat flow from Pollack et al. (1991), ranging from 0 (white) to >300 mW/m² (black).

of 5% was imposed. See the GSA Data Repository[1] for details of our inversion procedure.

Multiple inverse solutions were obtained at 10 km nominal resolution, using a range of prior one-dimensional models and varying degrees of smoothing. The preferred solution (model 1; Figs. 2 and 3) used a 200 Ωm half space as the prior, and fit the data to a normalized root mean square misfit of 1.89. We also discuss results from two alternative models (models 2 and 3, shown in the Data Repository) in the following section.

RESULTS

The most striking feature in all of the inverse solutions is a large, interconnected conductive body extending from the Yellowstone caldera at least 200 km to the southwest, roughly parallel to the direction of North America absolute motion (Figs. 2C and 3A). The depth to the top of this conductor varies from 30 to 60 km along the SRP, except in localized areas, including directly beneath Yellowstone caldera, where it reaches into the upper crust (Fig. 3A), and around the edges of the eastern SRP where it shallows to 18 km or so (Figs. 2A and 3B). The thickness of the most pronounced conductive area is 30–40 km, mostly in the uppermost mantle, and all within 80–100 km of the surface. To the east, the mantle is significantly more resistive, over 600 Ωm. At greater depths beneath the study area the upper mantle has moderately low resistivity (100 Ωm or less).

Crustal thickness beneath the eastern SRP and Yellowstone is inferred to be 40–50 km (Yuan et al., 2010), with the thickest crust directly beneath Yellowstone. Thinner crust surrounds the SRP, except to the east, beneath the Rocky Mountains. The vertically integrated conductivity (conductance; SI unit Siemens; S) of the lower crust (16–42 km) is highly variable in the inverse solution, ranging from ~80 to over 10,000 S beneath and around the SRP, and averaging ~1000 S. The average conductance at 42–80 km is over 3000 S beneath the SRP, reducing to 30–300 S in the Wyoming craton and directly beneath Yellowstone.

Depth resolution of the MT data is limited, both by the diffusive propagation of the electromagnetic fields in the conducting Earth, and by the distorting effects of near-surface heterogeneity. Indeed, assuming a more conductive mantle a priori results in conductive features that, while very similar in plan view, are shifted upward by up to 10 km (model 2, shown in Figs. DR1 and DR2 in the Data Repository). We thus must entertain the possibility that the low resistivities imaged at the top of the mantle in model 1 might actually be above the Moho. To test this, we ran the inversion using a prior model in which the crust was less resistive (60 Ωm) than the upper mantle (200 Ωm), thus pushing the low resis-
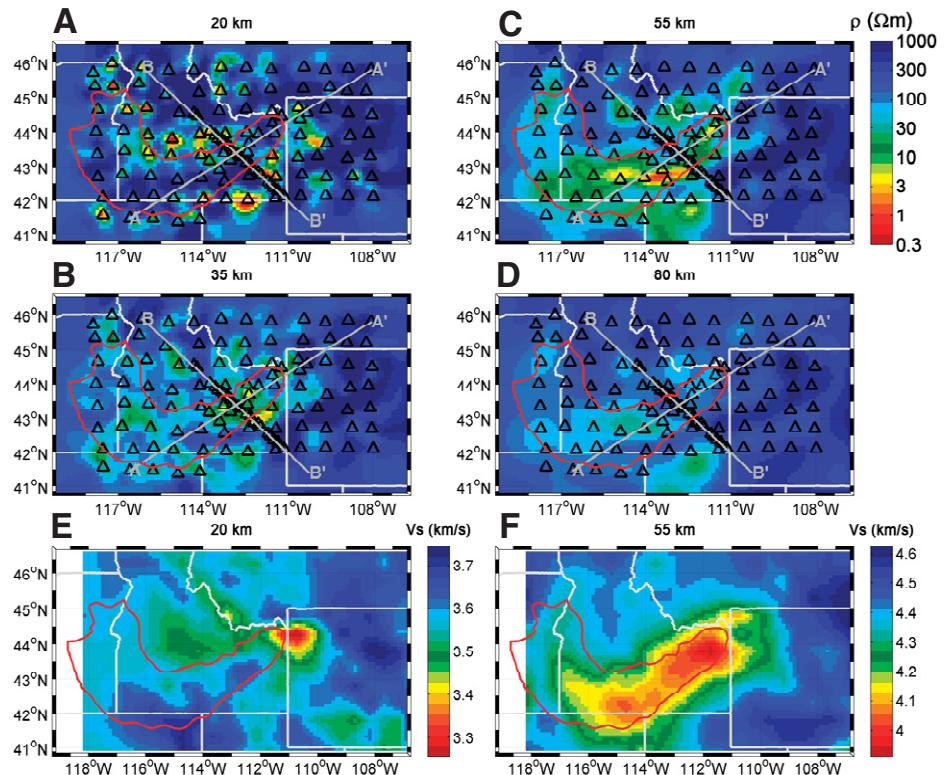

Figure 2. A-D: Preferred inverse model at representative depths. Lines indicate locations of profiles A–A′ and B–B′ shown in Figure 3. E-F: Seismic surface-wave velocity model of Yang et al. (2011) plotted at mid-crustal (20 km) and uppermost mantle (55 km) depths and interpolated to our grid for easier comparison. The contours of the Snake River Plain are plotted in red for reference.
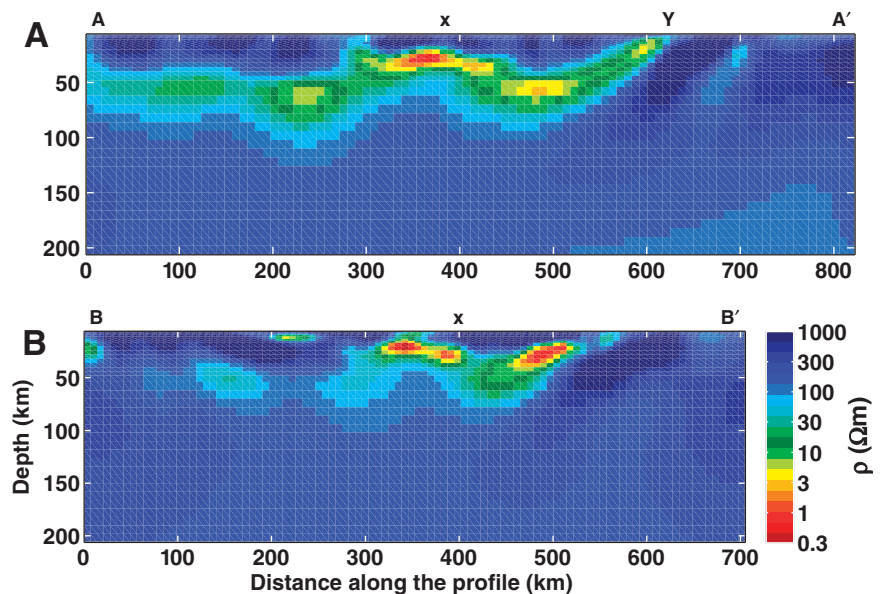

Figure 3. Cross sections from the preferred model along (A–A′) and across (B–B′) the eastern Snake River Plain. x—point of profile intersection; Y—Yellowstone caldera.

tivities into the crust as much as possible while still fitting the data adequately. The resulting inverse solution (model 3; Figs. DR3 and DR4) is noticeably rougher and has excessively conductive crust, averaging ~3000 S below the SRP, with peak values exceeding 10,000 S. Such high

conductivities are difficult to explain other than with free saline fluids distributed throughout the mid- to lower crust, an inference which is difficult to reconcile with seismic surface wave studies that reveal normal to fast lower crustal velocities in this area (Gao et al., 2011; Yang et

al., 2011; see also Fig. 2E). Furthermore, even with much of the anomaly pushed into the crust, model 3 is still anomalously conductive at the top of the mantle, with an average conductance of roughly 1000 S between 42 and 80 km depths beneath the SRP. We thus conclude that the MT data require elevated conductivities at the top of the upper mantle. Resistivities average no more than 40 Ωm beneath the SRP, and we consider the much lower values found in model 1 (Figs. 2 and 3) to be more likely.

In all inverse solutions, the upper mantle below ~100 km is more resistive beneath the Wyoming craton than beneath the SRP, but a range of resistivities, from 30 to over 100 Ωm, is recovered beneath the SRP depending on the prior model and regularization (Figs. DR3 and DR4). We conclude that deeper structures are shielded and confounded by the highly conductive and inhomogeneous crust and lithosphere, and thus concentrate our discussion on the lower crustal and uppermost mantle inhomogeneities that are resolved robustly.

DISCUSSION

Depth of Conductive Layers

High conductivities near the Moho have frequently been observed in the western United States, but these have most often been interpreted to be in the lower crust. For example, in the eastern Great Basin (Wannamaker et al., 2008) and the Pacific Northwest (Patro and Egbert, 2008), integrated lower crustal conductances of 3000 S or more, imaged by MT data, have been interpreted as saline fluids and partial melt associated with magmatic underplating. Indeed, elevated lower crustal conductivities for the eastern SRP were previously inferred by Stanley et al. (1977) from wide-band (0.001–500 s) MT profile data. Based on one-dimensional inversion of data from 12 sites, Stanley et al. (1977) inferred a low resistivity (~1 Ωm) layer with the top at ~7–9 km directly beneath the Yellowstone caldera system, deepening to ~25 km beneath the Island Park caldera, and then slightly shallowing further to the southeast. This is very similar to the shape of the anomaly we image, although our preferred solution (model 1; Figs. 2 and 3) locates the top of the conductive zone somewhat deeper.

The data of Stanley et al. (1977) were restricted to periods below 500 s, and could not image below the first highly conductive layer encountered in the crust. At the longer periods we have used (up to 20,000 s), the electromagnetic fields penetrate this layer, allowing resolution of deeper structure. However, as the variations between the three models discussed here demonstrate, the MT data by themselves do not always precisely constrain depths to specific features. This depth ambiguity results largely from

the effects of near-surface conductive heterogeneity (Jones, 1988), which can distort electric fields, essentially multiplying impedances for each site by a different frequency-independent real factor. This translates into uncertainty in MT data amplitudes, which carry the information about depth and magnitude of a conductor. An extreme example of this ambiguity is perhaps provided by the recent study by Zhdanov et al. (2011), who inverted a subset of the USArray MT data considered here. Their interpretation emphasized a deep (~300 km), extremely conductive (1 Ωm or less) sub-horizontal mantle structure dipping to the southwest, with a footprint quite similar to the anomaly we image. However, Zhdanov et al. (2011) only fit phase data in their inversion, and these data provide little constraint on actual depths.

Correlation with the results from seismic imaging can reduce the depth uncertainties and allow us to choose among models that fit the MT data. The footprint of the conductive anomaly in all of models 1–3 coincides with that of the very prominent low in shear wave velocities inferred at the top of the mantle from surface wave tomography (Obrebski et al., 2010; Wagner et al., 2010; Gao et al., 2011; Yang et al., 2011; see also Fig. 2F). Although the low velocities extend to greater depth than the conductive anomaly seen in even model 1 (200 km versus 100 km), peaks in the seismic and conductivity anomalies are both between 40 and 80 km depth, suggesting a common physical explanation, partial melt.

Implications for Melt Porosity

Accounting for the uncertainties associated with model smoothing and with the near-surface heterogeneity distortions, resistivities of 10 Ωm or below over large areas in the uppermost mantle are robustly resolved by the MT data (see the Results section). Observed shear-wave velocity anomalies of 6%–8% (Wagner et al., 2010) in the uppermost mantle beneath the SRP suggest a melt porosity of 1%–2% (Hammond and Humphreys, 2000). Laboratory measurements of basaltic melt in an olivine matrix (Yoshino et al., 2010) suggest that ~1% melt results in bulk resistivities of 2–10 Ωm, when extrapolated to temperatures of 1350–1450 °C, appropriate for the SRP lithosphere (Leeman et al., 2009). These results are consistent with complete wetting of grain boundaries and a melt resistivity of roughly 0.1 Ωm (at 1350 °C). Other studies (Ni et al., 2011) have found somewhat higher values for resistivity of dry basaltic melts, 0.2–0.3 Ωm at 1350–1450 °C. Based on the Hashin-Shtrikman upper bound, this would require a melt fraction of ~3% for a bulk resistivity of 10 Ωm. Significantly lower resistivities are found just below the Moho (a few Ωm). Considering the possibility of imperfect melt connection, higher

melt fractions, or some other explanation might be required. Although erupted SRP basalts are relatively dry (no more than ~1 wt% water; Leeman et al., 2009; Till et al., 2010), as little as 0.5 wt% water could reduce melt resistivity by a factor of two (Ni et al., 2011). Variations in composition could also increase the conductivity of the melt phase (Roberts and Tyburczy, 1999).

CONCLUSIONS

The MT and seismic results are consistent with the presence of a few percent partial melt between 40 and 80 km, depths that would normally be considered mantle lithosphere. The spatial coincidence of this region with the Yellowstone hotspot track suggests that passage of the North American plate over the plume has resulted in significant modification or thinning, perhaps leaving little or no lithospheric root beneath the eastern SRP. The presence of melt at the top of the upper mantle is consistent with the ongoing basaltic magmatism in the SRP, which has continued along the length of the hot-spot track since initial passage over the plume. Our images are also consistent with inferences from thermobarometry (Leeman et al., 2009) on shallow melt equilibration depths of 80–100 km or less, and with suggestions (Till et al., 2010) that similar basaltic magmas from the nearby High Lava Plains have equilibrated just below the Moho.

None of our inverse solutions show the SRP conductivity anomaly extending beneath Yellowstone at mantle depths. This stands in contrast to the seismic images (e.g., Wagner et al., 2010; Yang et al., 2011; see also Fig. 2F), which show substantial slow anomalies in the mantle immediately beneath Yellowstone. Both melt and high temperatures could contribute to these low seismic velocities, but the high resistivities rule out significant interconnection of any melt phase in the lithosphere directly beneath Yellowstone. Possibly the cratonic lithosphere in this area is largely intact, and still too thick to allow decompression melting (Leeman et al., 2009). In this scenario, the seismic anomaly would have a purely thermal explanation, with the lithosphere heated by a deep plume source. Alternatively, melt may be present in the lithosphere beneath Yellowstone, but at too low a concentration to be interconnected. Indeed, elevated temperatures beneath the active volcanic center would result in greater permeability, allowing magma to ascend to shallower depths and pool in the crust, instead of collecting in the mantle lithosphere, as beneath the SRP. We thus speculate that little melt is entering the system from below at present, perhaps due to intermittency of supply (as suggested by the apparent discontinuity with depth of the seismically imaged plume; e.g., James et al., 2011), while melt from earlier plume activity has mostly already ascended into the shallow crust, leaving behind only isolated

pockets of residual melt in the mantle lithosphere and lower crust. These would be effective at reducing seismic shear wave velocities (in conjunction with elevated temperatures), but would not significantly reduce resistivity.

High conductivities occur at mid-crustal levels (e.g., Fig. 2A) almost exclusively around the edges of the SRP. In cross section, these shallower features connect to the deeper conductive structure below the Moho (Fig. 3B), much as the shallow Yellowstone caldera conductor dips to the southwest and connects into the deeper anomaly (Fig. 3A). This suggests that melt, and perhaps also fluids exsolved by magmatic underplating, ascend into the crust preferentially around the edges of the generally impermeable SRP. We note the coincidence of these mid-crustal low resistivities with the "tectonic parabola" (e.g., Humphreys et al., 2000) of late Cenozoic normal faults, which may help to provide a preferred pathway for fluid or melt migration. Note also that the highest heat flows in this region occur around the edges of the SRP, again coincident with the mid-crustal conductive anomalies (Pollack et al., 1991; see also Fig. 1), and that shear wave velocities are reduced in this area at 20 km depth (see Fig. 2F).

Finally, we emphasize that the MT data provide at best weak constraints on deeper structure. The vertical seismic anomaly inferred (Yuan and Dueker, 2005; Obrebski et al., 2010) to be the mantle plume would likely represent only a thermal anomaly of roughly 125–150 °C (Leeman et al., 2009), at depths below 100 km or so. This excess temperature would increase electrical conductivity of dry olivine, but only modestly compared to the effects of fluids and melt. Such a relatively subtle signal would be challenging to resolve given the highly variable features we image at shallower depths.

In summary, our conductivity images suggest a more complex pattern of melt beneath the SRP and Yellowstone than would be expected from a continuously supplied, classical mantle plume with head sheared to the southwest by North American plate motion. Collection of partial melts at the base of the SRP province, inferred from the MT data, can perhaps explain some of the distinct features of SRP and Yellowstone magmatism.

ACKNOWLEDGMENTS

REFERENCES CITED

Christiansen, R.L., Foulger, G.R., and Evans, J.R., 2002, Upper-mantle origin of the Yellowstone hotspot: Geological Society of America Bulletin, v. 114, p. 1245–1256, doi:10.1130/0016-7606(2002)114<1245:UMOOTY>2.0.CO;2.

Egbert, G. D., and Kelbert, A., 2012, Computational Recipes for Electromagnetic Inverse Problems: Geophysical Journal International, doi:10.1111/j.1365-246x.2011.05347.x.

Gao, H., Humphreys, E.D., Yao, H., and van der Hilst, R.D., 2011, Crust and lithosphere structure of the northwest U.S. with ambient noise tomography: Terrane accretion and Cascade arc development: Earth and Planetary Science Letters, v. 304, p. 202–211, doi:10.1016/j.epsl.2011.01.033.

Geist, D., and Richards, M., 1993, Origin of the Columbia Plateau and Snake River plain: Deflection of the Yellowstone plume: Geology, 21, 789-+. doi:10.1130/0091-7613(1993)021<0789:OOTCPA>2.3.CO;2

Hadley, D.M., Stewart, G.S., and Ebel, J.E., 1976, Yellowstone: Seismic Evidence for a Chemical Mantle Plume: Science, v. 193, p. 1237–1239, doi:10.1126/science.193.4259.1237.

Hammond, W.C., and Humphreys, E.D., 2000, Upper mantle seismic wave velocity: Effects of realistic partial melt geometries: Journal of Geophysical Research, v. 105, p. 10,975–10,986, doi:10.1029/2000JB900041.

Humphreys, E.D., Dueker, K.G., Schutt, D.L., and Smith, R.B., 2000, Beneath Yellowstone: evaluating plume and nonplume models using teleseismic images of the upper mantle: GSA Today, v. 10, p. 1–7.

James, D.E., Fouch, M.J., Carlson, R.W., and Roth, J.B., 2011, Slab fragmentation, edge flow and the origin of the Yellowstone hotspot track: Earth and Planetary Science Letters, doi:10.1016/j.epsl.2011.09.007.

Jones, A.G., 1988, Static shift of magnetotelluric data and its removal in a sedimentary basin environment: Geophysics, v. 53, p. 967–978, doi:10.1190/1.1442533.

Leeman, W.P., Schutt, D.L., and Hughes, S.S., 2009, Thermal structure beneath the Snake River Plain: Implications for the Yellowstone hotspot: Journal of Volcanology and Geothermal Research, v. 188, p. 57–67, doi:10.1016/j.jvolgeores.2009.01.034.

Ni, H., Keppler, H., and Behrens, H., 2011, Electrical conductivity of hydrous basaltic melts: Implications for partial melting in the upper mantle: Contributions to Mineralogy and Petrology, v. 162, doi:10.1007/s00410-011-0617-4.

Obrebski, M., Allen, R.M., Xue, M., and Hung, S.-H., 2010, Slab-plume interaction beneath the Pacific Northwest: Geophysical Research Letters, v. 37, p. L14305, doi:10.1029/2010GL043489.

Patro, P.K., and Egbert, G.D., 2008, Regional conductivity structure of Cascadia: Preliminary results from 3D inversion of USArray transportable array magnetotelluric data: Geophysical Research Letters, v. 35, p. L20311, doi:10.1029/2008GL035326.

Pollack, H.N., Hurter, S.J., and Johnson, J.R., 1991, The New Global Heat Flow Compilation: Ann Arbor, Michigan, Department of Geological Sciences, University of Michigan, Technical Report.

Roberts, J.J., and Tyburczy, J.A., 1999, Partial-melt electrical conductivity: Influence of melt composition: Journal of Geophysical Research, v. 104, B4, doi:10.1029/1998JB900111.

Stanley, W.D., Boehl, J.E., Bostick, F.X., and Smith, H.W., 1977, Geothermal significance of magnetotelluric sounding in the eastern Snake River Plain-Yellowstone region: Journal of Geophysical Research, v. 82, p. 2501–2514, doi:10.1029/JB082i017p02501.

Tian, Y., Zhou, Y., Sigloch, K., Nolet, G., and Laske, G., 2011, Structure of North American mantle constrained by simultaneous inversion of multiple-frequency SH, SS, and Love waves: Journal of Geophysical Research, v. 116, p. B02307, doi:10.1029/2010JB007704.

Till, C., Grove, T., and Carlson, R., 2010, Message from the Moho: Petrologic clues to the origin of Quaternary basaltic lavas from oregon's High Lava Plains: Geological Society of America Abstracts with Programs, v. 42, no. 5, p. 343.

Wagner, L., Forsyth, D.W., Fouch, M.J., and James, D.E., 2010, Detailed three-dimensional shear wave velocity structure of the northwestern United States from Rayleigh wave tomography: Earth and Planetary Science Letters, v. 299, p. 273–284, doi:10.1016/j.epsl.2010.09.005.

Wannamaker, P.E., Hasterok, D.P., Johnston, J.M., Stodt, J., Hall, D.B., Sodergren, T.L., Pellerin, L., Maris, V., Doerner, W.M., Groenewold, K., and Unsworth, M.J., 2008, Lithospheric dismemberment and magmatic processes of the Great Basin-Colorado Plateau transition, Utah, implied from magnetotellurics: Geochemistry Geophysics Geosystems, v. 9, p. 1–38, doi:10.1029/2007GC001886.

Yang, Y., Shen, W., and Ritzwoller, M.H., 2011, Surface wave tomography on a large-scale seismic array combining ambient noise and teleseismic earthquake data: Earth Science, v. 24, p. 55–64, doi:10.1007/s11589-011-0769-3.

Yoshino, T., Laumonier, M., McIsaac, E., and Katsura, T., 2010, Electrical conductivity of basaltic and carbonatite melt-bearing peridotites at high pressures: Implications for melt distribution and melt fraction in the upper mantle: Earth and Planetary Science Letters, v. 295, p. 593–602, doi:10.1016/j.epsl.2010.04.050.

Yuan, H., and Dueker, K., 2005, Teleseismic P-wave tomogram of the Yellowstone plume: Geophysical Research Letters, v. 32, p. L07304, doi:10.1029/2004GL022056.

Yuan, H., Dueker, K., and Stachnik, J., 2010, Crustal structure and thickness along the Yellowstone hot spot track: Evidence for lower crustal outflow from beneath the eastern Snake River Plain: Geochemistry Geophysics Geosystems, v. 11, p. Q03009, doi:10.1029/2009GC002787.

Zhdanov, M.S., Smith, R.B., Gribenko, A., Cuma, M., and Green, M., 2011, Three-dimensional inversion of large-scale EarthScope magnetotelluric data based on the integral equation method: Geoelectrical imaging of the Yellowstone conductive mantle plume: Geophysical Research Letters, v. 38, p. L08307, doi:10.1029/2011GL046953.